J Biosci Vol. 42, No. 3, September 2017, pp. 417–425
DOI: 10.1007/s12038-017-9701-x

Targeting cleavage and polyadenylation specific factor 1 via shRNA inhibits cell proliferation in human ovarian cancer

Beiguang Zhang[1], Ying Liu[1], Donghui Liu[1] and Lei Yang[2]*

[1]*Department of Intervention Therapy, Jilin Cancer Hospital, Changchun, Jilin, China*

[2]*Department of Radiology, Jilin Cancer Hospital, Changchun, Jilin, China*

**Corresponding author (Email, yanglei_jilin@163.com)*

MS received 9 April 2017; accepted 1 July 2017; published online 27 July 2017

Cleavage and polyadenylation specificity factor 1 (CPSF1), a member of CPSF complex, has been reported to play a key role in pre-mRNA 3′-end formation, but its possible role in ovarian cancer remains unclear. In the present study, we found the mRNA level of CPSF1 was overexpressed in ovarian cancer tissues using Oncomine Cancer Microarray database. Then the loss-of-function assays, including CCK-8, colony formation and flow cytometry assays, were performed to determine the effects of CPSF1 on cell viability, proliferation, cell cycle and apoptosis of human ovarian cancer cell lines (SKOV-3 and OVCAR-3). The results indicated that depletion of CPSF1 suppressed cell viability, impaired colony formation ability, induced cell cycle arrest at G0/G1 phase and promoted cell apoptosis in ovarian cancer cells. Furthermore, knockdown of CPSF1 upregulated the expression of cleaved caspase-3 and PARP and downregulated CDK4/cyclin D1 expression. These data suggested that CPSF1 could promote ovarian cancer cell growth and proliferation *in vitro* and its depletion might serve as a potential therapeutic target for human ovarian cancer.

Keywords. Apoptosis; cell cycle; cell proliferation; CPSF1; ovarian cancer

1. Introduction

Ovarian cancer is one of the most lethal gynecologic malignancies and ranks the fifth leading cause of cancer-related deaths in women worldwide (Heintz *et al.* 2003; Siegel *et al.* 2016). It was estimated that the mortality rate of ovarian cancer has reached 140,200 per year along with higher annual incidence rate (Jemal *et al.* 2011). A key factor is a majority of patients are not diagnosed until an advanced stage, resulting in less than 25% 5-year survival rate (Legge *et al.* 2005; Karst and Drapkin 2010). Therefore, a better understanding of initiation and progression mechanisms of ovarian cancer is critical for development of clinical diagnosis and treatment for ovarian cancer.

Cleavage and polyadenylation specific factor (CPSF) is one member of multiple subunit factors required for a site-specific cleavage, which is involved in most cases eukaryotic pre-messenger(m)RNA 3′-end process (Murthy and Manley 1995). It is composed of CPSF1, CPSF2, CPSF3, CPSF4 and Fip1 (Kiefer *et al.* 2009). These mRNA 3′-ends maturation factors have been reported to be closely associated with the progression of multiple human cancers functioning as tumour suppressors (Kleiman and Manley 2001; Rozenblatt-Rosen *et al.* 2009) or oncogenic factors (Topalian *et al.* 2001; Cools *et al.* 2004; Gotlib *et al.* 2004; Aragaki *et al.* 2011). As the largest component of the CPSF complex, CPSF1 (alternatively known as CPSF160) is located in the nucleus and plays an essential role in determining the specificity and efficiency of the 3′-end processing of a subset of pre-mRNAs by recognizing the AAUAAA sequence (Keller *et al.* 1991; Danckwardt *et al.* 2008; Yang and Doublie 2011). Previous study has shown that defects of mRNA processing contributes to an increasing number of human hematopoietic diseases (Steinman 2007). Notably, there is recent evidence that CPSF1 is essential for hematopoietic stem cell (HSC) survival and differentiation in zebrafish (Bolli *et al.* 2011). However, its potential role in tumours has not been fully investigated due to a lack of data regarding CPSF1 expression and tumour cell proliferation.

In the present study, we investigated the potential role of CPSF1 in ovarian cancer *in vitro*. Using the Oncomine database (*www.oncomine.org*), we showed CPSF1 is commonly upregulated in ovarian cancer tissues. Then by using shRNA targeting CPSF1, we demonstrated CPSF1 is required for the cell growth and proliferation of ovarian cancer cells via affecting cell cycle progression and apoptotic pathway, which might help develop a new treatment approach for human ovarian cancer.

2. Materials and methods

2.1 *Oncomine gene expression analysis*

To investigate the expression pattern of CPSF1 in ovarian cancer, the expression level of CPSF1 genes was first analysed in ovarian cancer tissues using microarray gene expression datasets derived from the Oncomine database (*https://www.oncomine.org/*). Briefly, Data Type was mRNA, the Cancer Type was defined as ovarian cancer, and Analysis Type was Cancer versus Normal Analysis.

2.2 *Tissue specimen and cell lines*

Total 15 pairs of ovarian cancer and adjacent non-tumour tissues were collected from patients with ovarian cancer who underwent surgical resection at Department of Oncology, Jilin Cancer Hospital. The abscised tissues were immediately stored at −80°C and then subjected to quantitative real-time PCR (qRT-PCR) and Western blotting analysis. All participants wrote the informed consent and this research was approved by Ethics Committee of Jilin Cancer Hospital, China.

Ovarian cancer cell lines, SKOV-3 and OVCAR-3 were provided from Chinese Academy of Sciences Cell Bank (Shanghai, China) and cultured in RPMI 1640 medium (Life Technologies) supplemented with 10% fetal bovine serum (FBS, Hyclone), 100 μg/mL streptomycin sulfate and 100 U/mL penicillin (Life Technologies). These two cell lines were maintained in a humidified incubator containing 5% CO_2 at 37°C.

2.3 *Lentiviral vector construction and transfection*

Two short hairpin RNAs (shRNAs) target sequence (shRNA-1 and shRNA-2) for CPSF1 gene were synthesized by Shanghai GenePharma Co., Ltd, to deplete the expression of CPSF1 in ovarian cancer cells. A scrambled shRNA was used as a negative control. These shRNA oligos were cloned into the pLKO.1 vector (Addgene) between *AgeI* and *EcoRI* site and indicated as shCPSF1-1, shCPSF1-2 and shCon. Then combinant lentivirus was generated by co-transfecting shRNA plasmids and pHelper plasmids into HEK293Tcells using Lipofectamine 2000 (Invitrogen) according to the manufacturer's instruction. For cell transfection, SKOV-3 and OVCAR-3 cells were seeded in six-well plates and transfected with the constructed lentivirus containing shCPSF1-1, shCPSF1-2 or shCon at a multiplicity of infection (MOI) of 60. At 48 h after transfection, the knockdown efficiency was determined at mRNA and protein levels, respectively.

2.4 *Quantitative real time PCR (qRT-PCR) analysis*

Total RNA was collected from tissues and cells by Trizol reagent (Invitrogen, Carlsbad, CA) and 1 μg of total RNA was used to synthesize cDNA by use of the SuperScript® III First-Strand Synthesis System (Invitrogen, Carlsbad, CA). The primer sequences were as follows: CPSF1 (forward): 5′-TGACAGAATCACGCATTAACTTTT-3′ CPSF1 (reverse): 5′-CAACATGAACGACATGGTCA-3′; β-actin (forward): 5′-GTGGACATCCGCAAAGAC-3′, β-actin (reverse): 5′-AAAGGGTGTAACGCAACTA-3′. The β-actin was used as the internal reference control. The qRT-PCR was performed as described in the SYBR Green PCR Master Mix (Applied Biosystems) on CFX96 Real-Time System (BIO-RAD)using the following procedure: denaturation at 95°C for 2 min, 40 cycles at 95°C for 15 s, and annealing and extension at 60°C for 30 s. The $2^{-\Delta\Delta Ct}$ method was used to calculate the mRNA expression level of CPSF1.

2.5 *Western blotting*

Total proteins from tissues and cells were extracted using RIPA lysis buffer (Beyotime, China) and quantified by BCA protein assay (Beyotime, China). Forty micrograms of total protein were separated on 10% SDS-PAGE gel and then transferred to a PVDF membrane. The membrane was then blocked with 5% nonfat milk Tris buffer for 1 h and then incubated overnight with antibodies against CPSF1 (11504-1-AP, Proteintech Group, Inc., USA), CDK4 (11026-2-AP, Proteintech Group, Inc., USA), Cyclin D1 (60186-1-1g, Proteintech Group, Inc., USA), PARP (#9542, Cell signaling Technology, USA), caspase-3 (19677-1-AP, Proteintech Group, Inc., USA) and GAPDH (10494-1-AP, Proteintech Group, Inc., USA). Then membranes were washed with TBST three times, and then further incubated with horseradish peroxidase (HRP)-conjugated corresponding secondary antibody for 2 h. After rinsing with Tris buffer for 30 min, the immunoblots were visualized by enhanced chemiluminescence (ECL, Beyotime, China). All antibodies were purchased from Proteintech, USA. GAPDH was used as the Western blot loading control.

2.6 *CCK-8 assay*

Ovarian cancer cells were plated into 96-well plates at an initial density of 3000 cells per well after transfection with shCon, shCPSF1-1 or shCPSF1-2. After transfection for 24, 48, 72 and 96 h, each well was added 10 μL of the CCK-8 solution (DOJINDO, Kumamoto, Japan) and incubated for 2 h. The absorbance at 450 nm was measured using a microplate reader.

2.7 *Clone formation assay*

Ovarian cancer cells, at a density of 500 cells per well, were spread out on a 6-well plate and cultured for 14 days to grow

natural colonies. When clones were macroscopic, each well was carefully rinsed twice with PBS, and fixed by 10% formaldehyde for 15 min, and stained with crystal violet for 30 s. Then, each well was washed with running water slowly and naturally air dried. The colonies (more than 50 cells per colony) were counted under the microscope.

2.8 *Flow cytometry analysis*

Flow cytometry analysis was performed to evaluate the effect of CPSF1 depletion on cell cycle progression and apoptosis in SKOV-3 cells. Cells for cell cycle analysis were collected, washed with ice-cold PBS, and fixed with ice-cold 70% (v/v) ethanol at 4°C overnight. Then, the cell pellets incubated with 0.1 mg/ml RNase I and 50 mg/mL propidium iodide (PI) at 37°C for 30 min. The percentage of the cells in G1, S, and G2–M phase were determined with a flow cytometer (BD, USA).

The apoptotic cells were detected with Annexin V-APC/7-AAD apoptosis detection kit according to the manufacturer's instruction (eBioscience, SanDiego, CA, USA). After the double staining, flow cytometry analysis was performed as mentioned above.

2.9 *Hoechst 33342 staining*

The apoptotic effect of CPSF1 depletion on ovarian cancer cells was analysed by blue fluorescent Hoechst 33342 dye (Life Technology, USA). Briefly, cells (1×10^5 cells/well) were seeded in 12-well plates after transfection, then washed twice with PBS, and stained with 10 μg/mL Hoechst 33342 for 15 min in dark at room temperature. Subsequently, apoptotic cells, which exhibited a bright blue fluorescence, were observed under a fluorescence microscope (Leica, German).

2.10 *Statistical analysis*

Statistical analysis and graphs presentation were performed with GraphPad Prism 6.0 software. Quantitative data were expressed as mean ± standard deviation (SD) of three repeated measurement data. Comparisons between two groups were conducted with Student's *t* test. $P<0.05$ was considered statistically significant.

3. Results

3.1 *CPSF1 was overexpressed in ovarian cancer tissues*

Using the Oncomine database (*www.oncomine.org*), CPSF1 mRNA levels were investigated in human ovarian cancer. As shown in figure 1A and B, CPSF1 mRNA expression was found significantly elevated in various ovarian cancer types, including ovarian clear cell, endometrioid, mucinous, and serous adenocarcinoma compared with that in normal tissues using Lu Ovarian Statistics (Lu *et al.* 2004) and Hendrix Ovarian Statistic datasets (Hendrix *et al.* 2006). Meanwhile, the expression of CPSF1 was remarkably increased in ovarian cancer tissues compared with the corresponding normalovary tissues in the data derived from the TCGA database *(https://tcga-data.nci.nih.gov/)* (figure 1C, P = 5.87E−4) and Bonome Ovarian Statistics (figure 1D, P = 2.59E−4) (Bonome *et al.* 2008).

To validate these observations, we examined the expression of CPSF1 in 15 pairs of ovarian cancer tissues and adjacent normal tissues using qRT-PCR and Western blotting analysis. As expected, the expression levels of CPSF1 mRNA were significantly increased in ovarian carcinoma tissues compared with normal tissues (figure 1E, $P<0.001$). Similarly, representative 8 pairs of tissues also indicated that CPSF1 was obviously upregulated in ovarian cancer tissues at protein levels (figure 1F). Collectively, these data highlighted an upregulated expression of CPSF1 in ovarian cancer.

3.2 *Lentivirus-mediated shRNA suppressed CPSF1 expression in ovarian cancer cells*

To assess the functional role of CPSF1 in ovarian cancer *in vitro*, we transfected shCPSF1-1 or shCPSF1-2 into ovarian cancer cell lines, SKOV-3 and OVCAR-3 to specific deplete the endogenous expression of CPSF1. Using qRT-PCR analysis, the knockdown efficiency was confirmed at mRNA levels. As shown in figure 2A and B, the mRNA level of CPSF1 was significantly reduced in both SKOV-3 and OVCAR-3 cells following shCPSF1-1 or shCPSF1-2 transfection ($P<0.001$). Moreover, the protein level of CPSF1 was decreased by shCPSF1-1 or shCPSF1-2, respectively (figure 2C and D, $P<0.001$). These analyses confirmed CPSF1 was specifically depleted by CPSF1 shRNA.

3.3 *Depletion of CPSF1 impaired cell viability and colony formation ability in ovarian cancer cells*

After confirming the higher knockdown efficiency of shCPSF1-1 or shCPSF1-2, we next investigated the effects of CPSF1 depletion on ovarian cancer cell proliferation, including cell viability and colony formation ability. CCK-8 assay indicated that the growth curve of SKOV-3 (figure 3A, $P<0.05$, $P<0.001$) and OVCAR-3 cells (figure 3B, $P<0.01$) was significantly dropped in both shCPSF1-1 and shCPSF1-

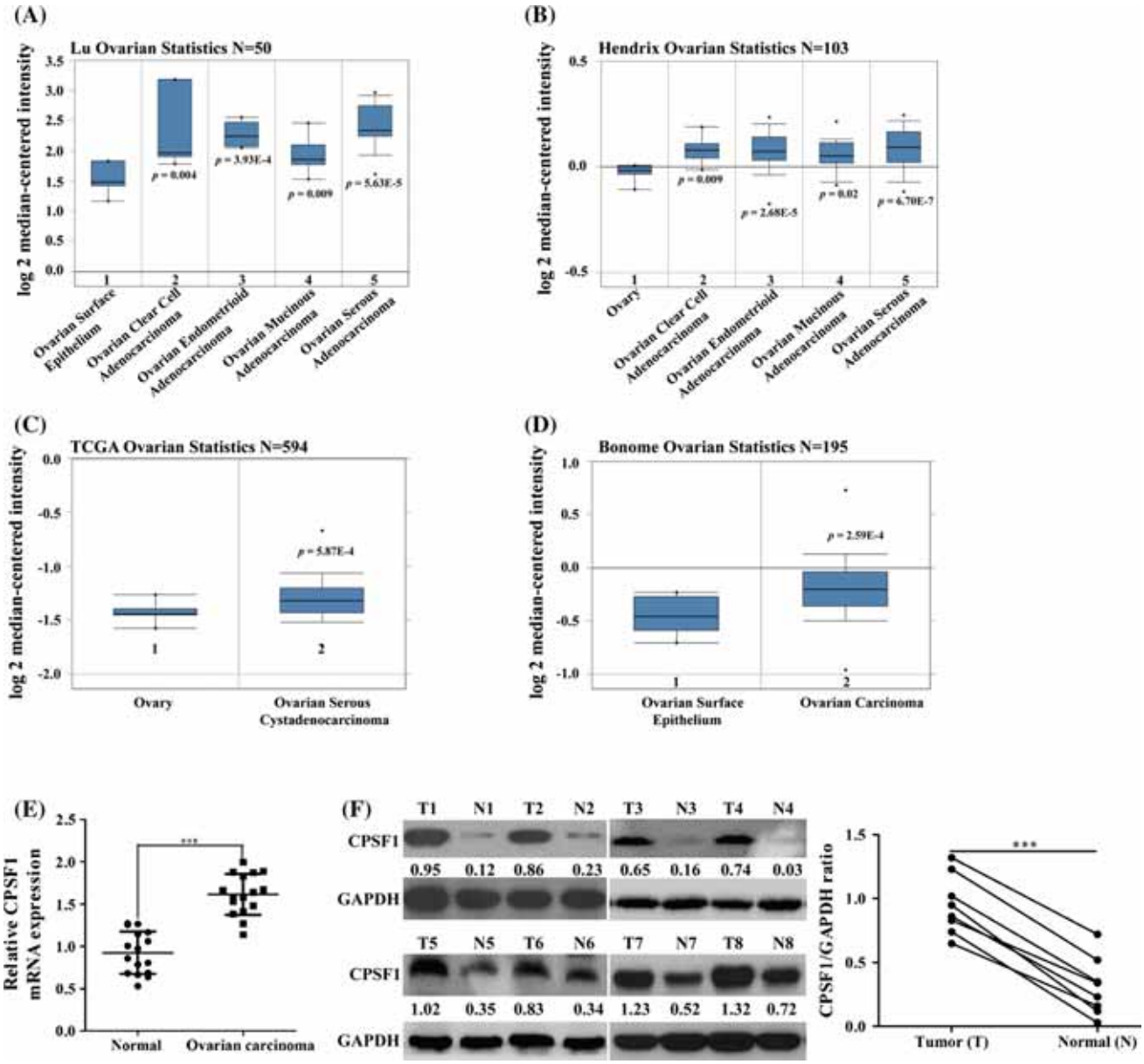

Figure 1. The expression of CPSF1 was significantly upregulated in ovarian cancer tissues. The mRNA expression of CPSF1 was analysed in Oncomine datasets including Lu Ovarian Statistics (**A**), Hendrix Ovarian Statistic datasets (**B**), TCGA Ovarian (**C**) and Bonome Ovarian Statistics (**D**). (**E**) Quantitative real-time PCR (qRT-PCR) analysis of CPSF1 mRNA in 15 paired ovarian cancer tissues. (**F**) Expression levels of CPSF1 protein in representative 8 paired ovarian cancer tissues by Western blotting. Quantitative data were expressed as mean ± standard deviation (SD) of three repeated measurement data. ***P<0.001 compared with normal tissues. N, adjacent noncancerous tissues, T, tumour tissues; GAPDH serves as an internal control.

2 groups than in shCon groups. Surprisingly, we found shCPSF1-1 could be more powerful in suppressing cell viability than shCPSF1-2 in these two ovarian cancer cell lines. Thus, shCPSF1-1 was chosen for the subsequent analysis. Colony formation assay showed a significant decreased in the colonies of CPSF1-1 depleted SKOV-3 (figure 3C, 191 ± 17 *vs*. 62 ± 28) and OVCAR-3 cells (figure 3D, 203 ± 24 *vs*. 72 ± 15) compared with their shCon cells (P<0.05). Based on these findings, we speculated that CPSF1 might be essential for ovarian cancer cell proliferation.

3.4 *Depletion of CPSF1 induced cell cycle arrest in ovarian cancer cells*

To better understand the positive role of CPSF1 in ovarian cancer cell proliferation, we analysed the cell cycle

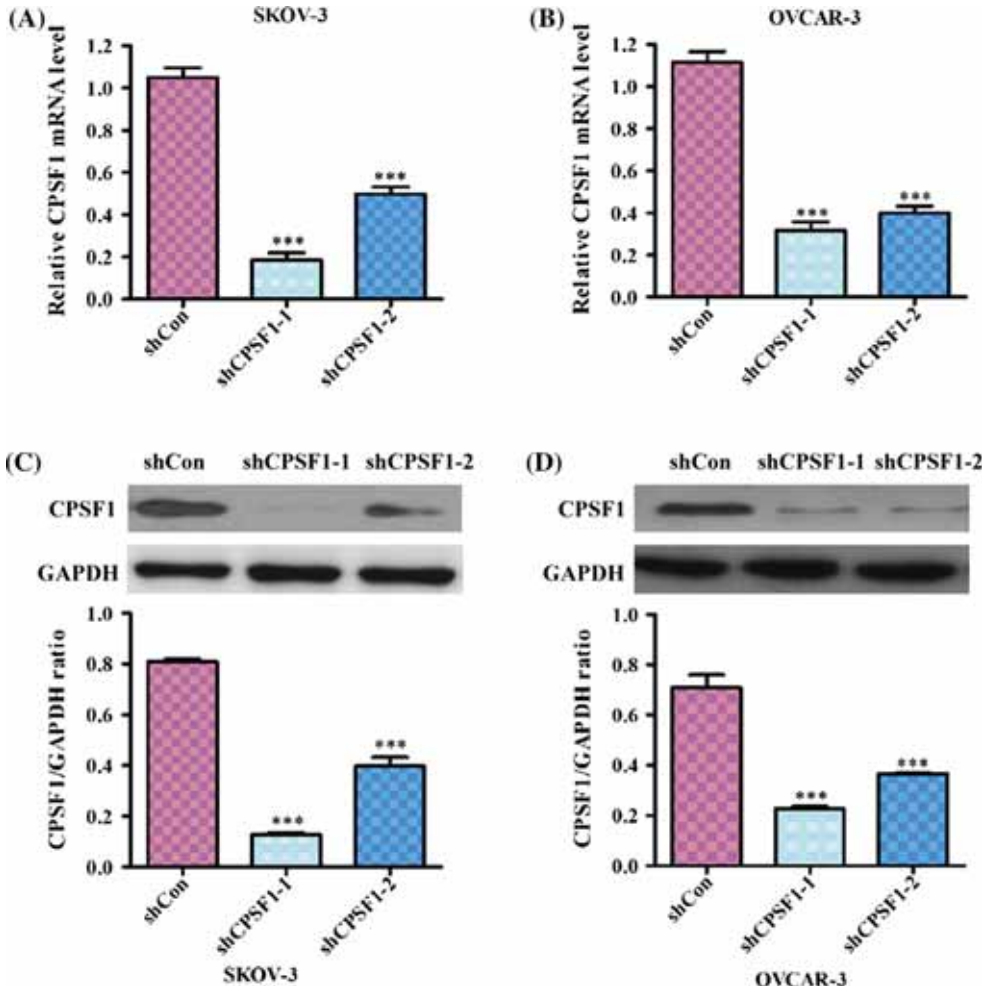

Figure 2. The expression of CPSF1 was specifically depleted by lentivirus-mediated shRNA. The mRNA levels of CPSF1 in SKOV-3 (**A**) and OVCAR-3 (**B**) cells with three transfections (shCon, shCPSF1-1, and shCPSF1-2) determined by qRT-PCR. The protein levels of CPSF1 in SKOV-3 (**C**) and OVCAR-3 (**D**) cells with three transfections (shCon, shCPSF1-1, and shCPSF1-2) determined by Western blotting. Quantitative data were expressed as mean ± standard deviation (SD) of three repeated measurement data. ***$P<0.001$ compared with shCon.

distribution of SKOV-3 cell after transfection with shCon or shCPSF1-1 using flow cytometry with PI staining (figure 4A). Quantitative analysis further demonstrated that SKOV-3 cells transfected with shCPSF1-1 showed apparent increases in the percentage of cells in G0/G1 phase, accompanied with significant decreases in the percentage of cells in S phase compared with cells transfected with shCon (figure 4B, $P<0.001$). Furthermore, we examined the expression of cell cycle-related proteins in CPSF1 depletion ovarian cancer cells. As depicted in figure 4C, depletion of CPSF1 led to a significantly decrease expression of cyclin-dependent kinase 4 (CDK4) and cyclin D1 ($P<0.001$). These results proved that depletion of CPSF1 caused cell cycle arrest at G0/G1 phase by inhibiting cell cycle regulatory factors.

3.5 *Depletion of CPSF1 increased ovarian cancer cell apoptosis*

We next investigated the involvement of CPSF1 in cell death of ovarian cancer cells by inhibiting CPSF1 expression with shRNAs. Hosechst 33342 staining was first used to examine the apoptotic SKOV-3 cells. The fluorescence images revealed obviously higher nuclear fragmentation, indicating apoptosis in shCPSF1-1 transfected SKOV-3 cells compared with shCon transfected controls (figure 5A). Moreover, flow cytometry with Annexin V/7-AAD double staining was performed to further confirmed pro-apoptotic effects of CPSF1 depletion in SKOV-3 cells. As shown in figure 5B and C, depletion of CPSF1 significantly increased early apoptotic cells (Annexin V+/7-AAD-) from 6.89% ± 0.2%

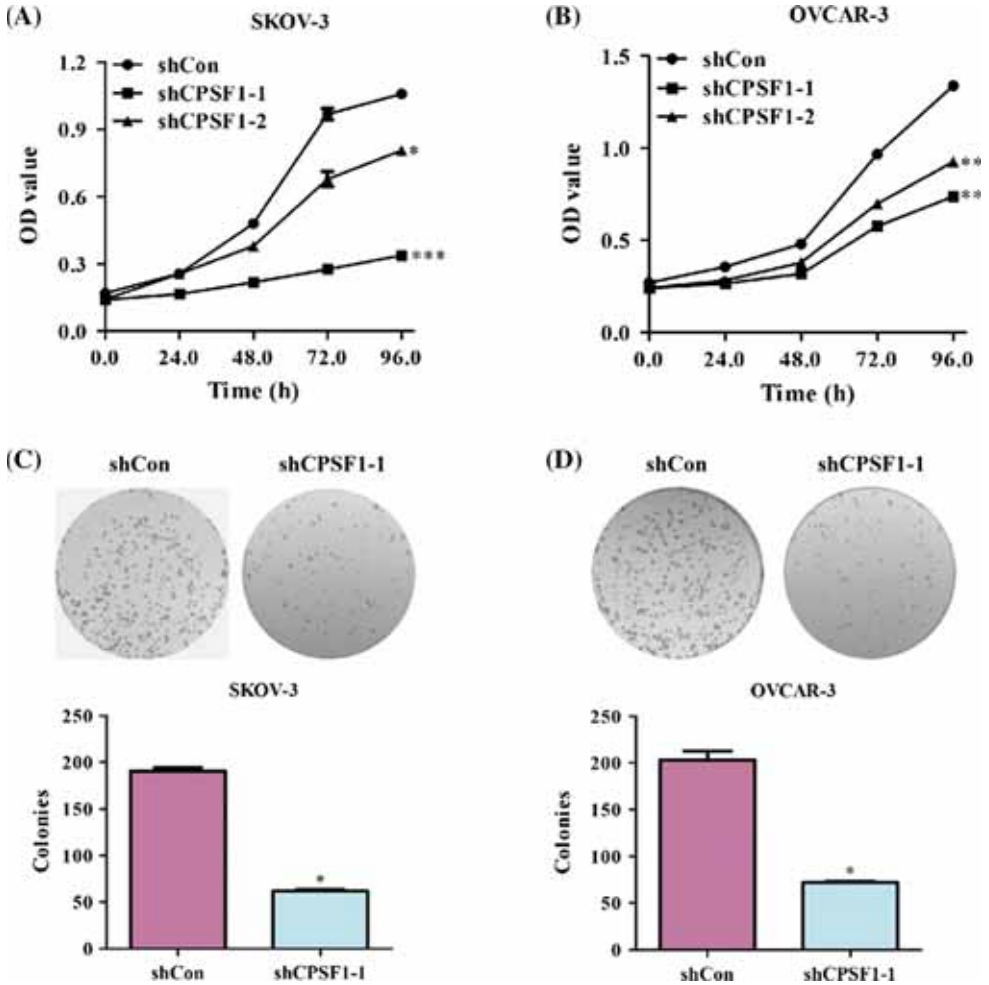

Figure 3. Depletion of CPSF1 suppressed cell proliferation in ovarian cancer. CCK-8 assay was performed to analyse cell viability in SKOV-3 (**A**) and OVCAR-3 (**B**) cells following three transfections (shCon, shCPSF1-1, and shCPSF1-2). The number of colonies were recorded and counted under the microscope in SKOV-3 (**C**) and OVCAR-3 (**D**) cells following two transfections (shCon and shCPSF1-1). Quantitative data were expressed as mean ± standard deviation (SD) of three repeated measurement data. *P<0.05, **P<0.01, ***P<0.001 compared with shCon.

to 16.32% ± 0.6% and late apoptotic cells (Annexin V+/7-AAD+) from 3.12% ± 0.4% to 8.41% ± 0.5% (P<0.001). Cleavage of caspase-3 and PARP were crucial markers for cell apoptosis. As described in figure 5D, the expression levels of cleaved caspase-3 and cleaved PARP protein were remarkably elevated in SKOV-3 cells after CPSF1 depletion. Therefore, these data supported that CPSF1 depletion had pro-apoptotic effects in ovarian cancer cells by activating the intrinsic apoptotic pathway.

4. Discussion

CPSF1, with a molecular weight of 160 kDa, has been reported to play a key role in pre-mRNA ‘6 formation by recognizing the AAUAAA signal sequence involved in the polyadenylation reaction. But the role and regulating mechanism of CPSF1 remains elusive in cancer. In our current study, we found that the expression of CPSF1 was significantly upregulated in ovarian cancer tissues by comparison with normal tissues. Moreover, the results from our *in vitro* experiments suggested that suppression of CPSF1 repressed cell proliferation, induced cell cycle G0/G1 phase arrest, and increased cell apoptosis in ovarian cancer, implying that it has a growth-promoting function.

It is known that pre-mRNA is subjected to mRNA processing in eukaryotes including capping, polyadenylation and splicing (Koga *et al.* 2013), in which CPSF plays an important role in its 3′-end-processing as the most rate-limiting step. CPSF1 belongs to the CPSF complex, whose other members are recently demonstrated to be deregulated in cancer. For example, CPSF3 is relevant for viral gene

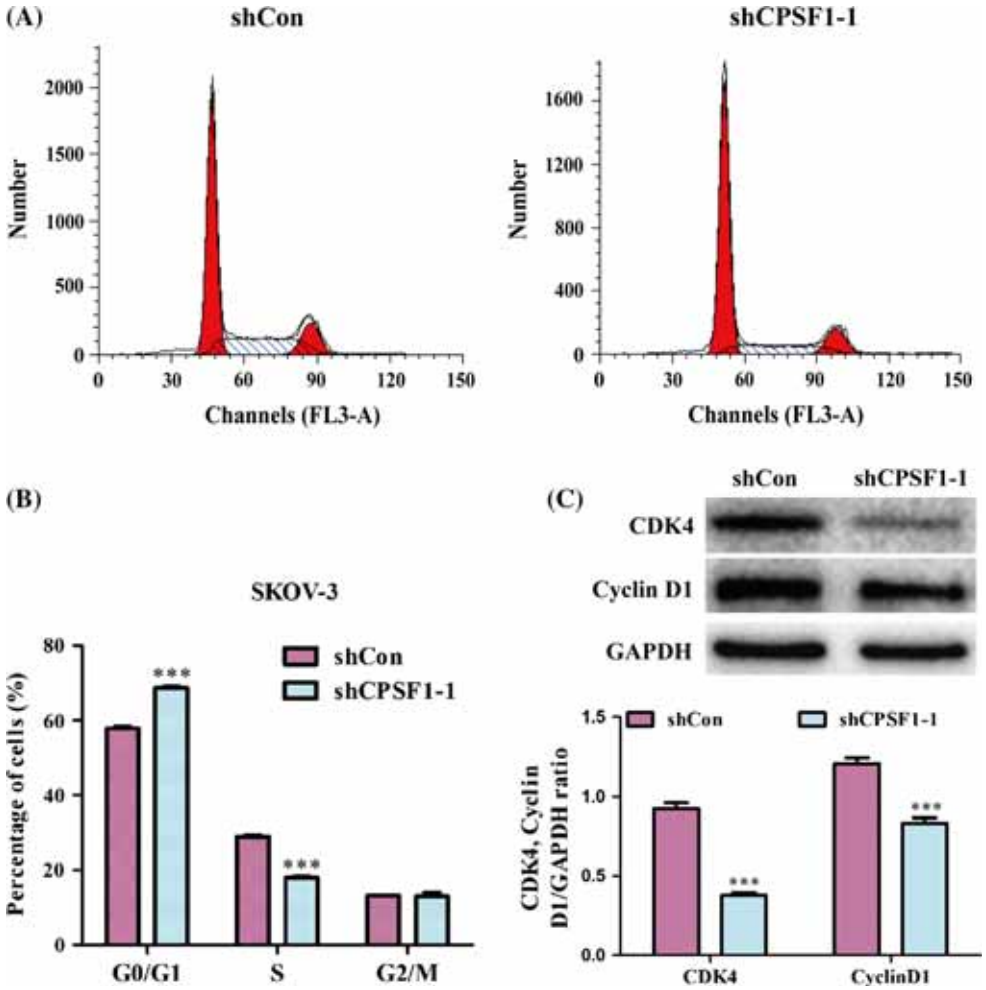

Figure 4. Depletion of CPSF1 arrested the cell cycle of ovarian cancer cells. (**A**) Flow cytometry with PI staining was used to determine the cell cycle distribution of SKOV-3 cells following two transfections (shCon and shCPSF1-1). (**B**) Statistical analysis of the percentage of cells in G0/G1, S and G2/M phases in SKOV-3 cells following two transfections (shCon and shCPSF1-1). (**C**) The expression levels of cell cycle-related proteins (CDK4 and Cyclin D1) were determined by Western blotting in SKOV-3 cells following two transfections (shCon and shCPSF1-1). Quantitative data of CDK4 and Cyclin D1 proteins were expressed as mean ± standard deviation (SD) of three repeated measurement data. ***P<0.001 compared with shCon.

expression, which could be increased by HIV-1 Tat protein, thereby contributing to HIV-1 pathogenesis by causing an increase in both cell and viral gene expression (Calzado *et al.* 2004). CPSF4 was highly expressed and its upregulation predicted poor prognosis in lung cancer patients. Furthermore, knockdown of CPSF4 inhibited the growth of lung cancer cells *in vitro* by simultaneous inactivation of the PI3K/AKT and MAPK signaling and activation of the caspase-dependent apoptotic pathways (Chen *et al.* 2013). Based these evidences, we could infer that CPSF1 might be a potential diagnostic or therapeutic target in ovarian cancer.

To investigate the underline molecular mechanisms, we examined cell cycle and apoptosis signaling pathway alteration. The results further revealed that knockdown of CPSF1 induced cell cycle arrest at G0/G1 phase through downregulating the expression of CDK4/Cyclin D1 complex. Consistent with our data, depletion of CPSF3 homologue causes the G0/G1 arrest of Hela cells (Dominski *et al.* 2005), indicating putative RNA processing factor, including CPSF1 affecting cell cycle regulation. Cyclin D1 is synthesized in G0/G1 phase and could activate of CDK4/CDK6 by forming the cyclin D1-CDK4 or cyclin D1-CDK6 complexes. Activation of CDK4 promotes DNA transcription, replication and repair, which is a key determinant that promote cell cycle progression (Ye *et al.* 2016). These results indicate that CDK4 and Cyclin D1 might be the downstream targets of CPSF1 in ovarian cancer. Furthermore, knockdown of CPSF1 enhanced apoptotic factors such as cleaved caspase-3 and PARP, resulting in an increase in apoptosis of ovarian cancer cells. These findings may conclude that

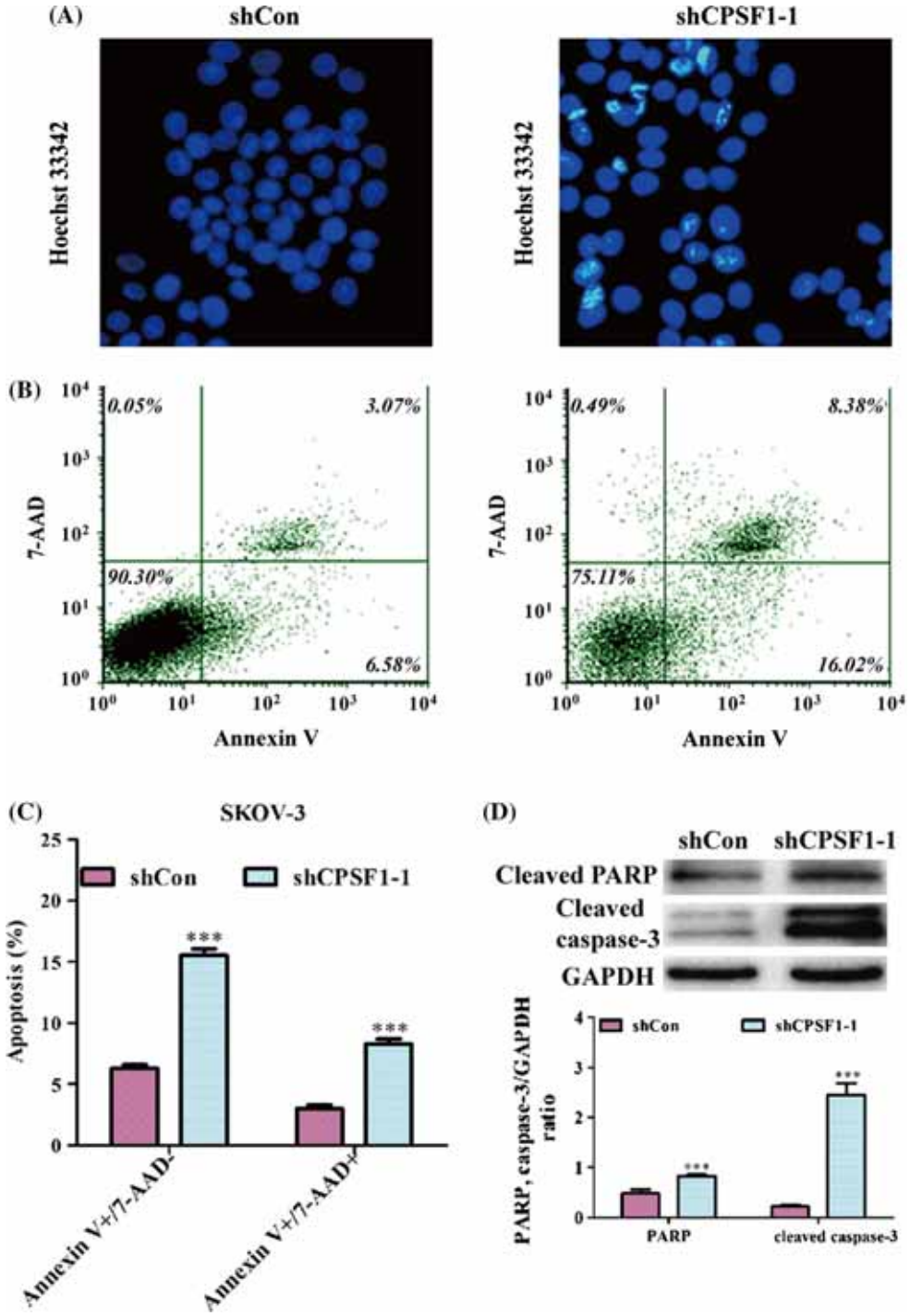

Figure 5. Depletion of CPSF1promoted cell apoptosis of ovarian cancer cells. (**A**) Morphological changes of SKOV-3 cells following two transfections (shCon and shCPSF1-1) using Hoechst 33342 fluorescence staining. (**B**) Flow cytometry with Annexin V/7-AAD double staining was used to measure apoptosis of SKOV-3 cells following two transfections (shCon and shCPSF1-1). (**C**) Statistical analysis of the early apoptotic (Annexin V+/7-AAD-) and late apoptotic cells (Annexin V+/7-AAD+) in SKOV-3 cells following two transfections (shCon and shCPSF1-1). (**D**) The expression levels of cleaved caspase-3 and PARP were determined by Western blotting in SKOV-3 cells following two transfections (shCon and shCPSF1-1). Quantitative data of cleaved caspase-3 and PARP proteins were expressed as mean ± standard deviation (SD) of three repeated measurement data. ***P<0.001 compared with shCon.

CPSF1 exert its growth-regulating effect, at least in part, by modulating the cell cycle and apoptotic regulation in ovarian cancer.

In summary, this study elucidated CPSF1 was significantly upregulated in ovarian cancer tissues. Through loss-of-function assays, we further demonstrated that knockdown of CPSF1 inhibits cell proliferation by inducing cell G0/G1 phase arrest and apoptosis. Although further detailed analyses are necessary to explore the exact mechanism underlying cell growth inhibition by CPSF1 knockdown, our results provide a rational for pharmacologic investigation of CPSF1 as a potential therapeutic target for ovarian cancer.

References

Aragaki M, Takahashi K, Akiyama H, Tsuchiya E, Kondo S, Nakamura Y and Daigo Y 2011 Characterization of a cleavage stimulation factor, 3' pre-RNA, subunit 2, 64 kDa (CSTF2) as a therapeutic target for lung cancer. *Clin. Cancer Res.* **17** 5889–5900

Bolli N, Payne EM, Rhodes J, Gjini E, Johnston AB, Guo F, Lee JS, Stewart RA, Kanki JP and Chen AT 2011 cpsf1 is required for definitive HSC survival in zebrafish. *Blood* **117** 3996–4007

Bonome T, Levine DA, Shih J, Randonovich M, Pise-Masison CA, Bogomolniy F, Ozbun L, Brady J, Barrett JC, Boyd J and Birrer MJ 2008 A gene signature predicting for survival in suboptimally debulked patients with ovarian cancer. *Cancer Res.* **68** 5478–5486

Calzado MA, Sancho R and Munoz E 2004 Human immunodeficiency virus type 1 Tat increases the expression of cleavage and polyadenylation specificity factor 73-kilodalton subunit modulating cellular and viral expression. *J. Virol.* **78** 6846–6854

Chen W, Guo W, Li M, Shi D, Tian Y, Li Z, Wang J, Fu L, Xiao X, Liu QQ, Wang S, Huang W and Deng W 2013 Upregulation of cleavage and polyadenylation specific factor 4 in lung adenocarcinoma and its critical role for cancer cell survival and proliferation. *PLoS One* **8** e82728

Cools J, Stover EH, Wlodarska I, Marynen P and Gilliland DG 2004 The FIP1L1-PDGFRalpha kinase in hypereosinophilic syndrome and chronic eosinophilic leukemia. *Curr. Opin. Hematol.* **11** 51–57

Danckwardt S, Hentze MW and Kulozik AE 2008. "3' end mRNA processing: molecular mechanisms and implications for health and disease. *EMBO J.* **27** 482–498

Dominski Z, Yang XC, Purdy M, Wagner EJ and Marzluff WF 2005 A CPSF-73 homologue is required for cell cycle progression but not cell growth and interacts with a protein having features of CPSF-100. *Mol. Cell Biol.* **25** 1489–1500

Gotlib J, Cools J, Malone JM 3rd, Schrier SL, Gilliland DG and Coutre SE 2004 The FIP1L1-PDGFRalpha fusion tyrosine kinase in hypereosinophilic syndrome and chronic eosinophilic leukemia: implications for diagnosis, classification, and management. *Blood* **103** 2879–2891

Heintz AP, Odicino F, Maisonneuve P, Beller U, Benedet JL, Creasman WT, Ngan HY and Pecorelli S 2003 Carcinoma of the ovary. *Int. J. Gynaecol. Obstet.* **83** 135–166

Hendrix ND, Wu R, Kuick R, Schwartz DR, Fearon ER and Cho KR 2006 Fibroblast growth factor 9 has oncogenic activity and is a downstream target of Wnt signaling in ovarian endometrioid adenocarcinomas. *Cancer Res.* **66** 1354–1362

Jemal A, Bray F, Center MM, Ferlay J, Ward E and Forman D 2011 Global cancer statistics. *CA Cancer J. Clin.* **61** 69–90

Karst AM and Drapkin R 2010 Ovarian cancer pathogenesis: a model in evolution. *J. Oncol.* **2010** 932371

Keller W, Bienroth S, Lang KM and Christofori G 1991 Cleavage and polyadenylation factor CPF specifically interacts with the pre-mRNA 3' processing signal AAUAAA. *EMBO J.* **10** 4241–4249

Kiefer H, Mizutani A, Iemura S, Natsume T, Ando H, Kuroda Y and Mikoshiba K 2009 Inositol 1,4,5-triphosphate receptor-binding protein released with inositol 1,4,5-triphosphate (IRBIT) associates with components of the mRNA 3' processing machinery in a phosphorylation-dependent manner and inhibits polyadenylation. *J. Biol. Chem.* **284** 10694–10705

Kleiman FE and Manley JL 2001 The BARD1-CstF-50 interaction links mRNA 3' end formation to DNA damage and tumor suppression. *Cell* **104** 743–753

Koga M, Satoh T, Takasaki I, Kawamura Y, Yoshida M and Kaida D 2013 U2 snRNP is required for expression of the 3' end of genes. *Plos One* **9** e98015

Legge F, Ferrandina G, Salutari V and Scambia G 2005 Biological characterization of ovarian cancer: prognostic and therapeutic implications. *Ann Oncol* **16**(Suppl 4) iv95–101

Lu KH, Patterson AP, Wang L, Marquez RT, Atkinson EN, Baggerly KA, Ramoth LR, Rosen DG, Liu J, Hellstrom I, Smith D, Hartmann L, Fishman D, Berchuck A, Schmandt R, Whitaker R, Gershenson DM, Mills GB and Bast RC Jr 2004 Selection of potential markers for epithelial ovarian cancer with gene expression arrays and recursive descent partition analysis. *Clin. Cancer Res.* **10** 3291–3300

Murthy KG and Manley JL 1995 The 160-kD subunit of human cleavage-polyadenylation specificity factor coordinates pre-mRNA 3'-end formation. *Genes Dev.* **9** 2672–2683

Rozenblatt-Rosen O, Nagaike T, Francis JM, Kaneko S, Glatt KA, Hughes CM, LaFramboise T, Manley JL and Meyerson M 2009 The tumor suppressor Cdc73 functionally associates with CPSF and CstF 3' mRNA processing factors. *Proc Natl Acad Sci U S A* **106** 755–760

Siegel RL, Miller KD and Jemal A 2016 Cancer statistics, 2016. *CA Cancer J. Clin.* **66** 7–30

Steinman RA 2007 mRNA stability control: a clandestine force in normal and malignant hematopoiesis. *Leukemia* **21** 1158–1171

Topalian SL, Kaneko S, Gonzales MI, Bond GL, Ward Y and Manley JL 2001 Identification and functional characterization of neo-poly(A) polymerase, an RNA processing enzyme overexpressed in human tumors. *Mol. Cell Biol.* **21** 5614–5623

Yang Q and Doublie S 2011 Structural biology of poly(A) site definition. Wiley Interdiscip. *Rev. RNA* **2** 732–747

Ye D, Luo H, Lai Z, Zou L, Zhu L, Mao J, Jacob T, Ye W, Wang L and Chen L 2016 ClC-3 chloride channel proteins regulate the cell cycle by up-regulating cyclin D1-CDK4/6 through suppressing p21/p27 expression in nasopharyngeal carcinoma cells. *Sci. Rep.* **6** 30276

Corresponding editor: Sorab Dalal